Combustion Improvement for Reducing Exhaust Emissions in a DI Diesel Engine

S. Jafarmadar[1,*] and M. Hosenzadeh[2]

[1] Assistant Professor, [2] Msc. Student, Mechanical Engineering Department, University of Urmia, Iran.

[*] s.jafarmadar@urmia.ac.ir

Abstract

This article investigates the improvement of operation characteristics and emissions reduction by means of creating an air-cell inside the piston body, exhaust gases re-circulating and insulating combustion chamber in a direct injection diesel engine simultaneously. The engine considered is a caterpillar 3401 which was modeled with an air-cell included as part of the piston geometry. This air-cell demonstrates that air injection in late combustion period can be effective in a significant reduction of Soot emission while cold EGR can be effective in reduction of NOx emission. Also for increasing of performance parameters, combustion chamber with air-cell is insulated. The analyses are carried out at part (75% of full load) and full load conditions at the same engine speed 1600 rpm.

The predicted results for mean in-cylinder pressure and emissions are compared to the corresponding experimental results and show good agreements. The obtained results indicate that creating the air-cell has a slight effect on improvement of performance parameters and it has significantly effect on Soot reduction. The air-cell decreases the Soot pollutant as a factor of two at both part and full load conditions. Also, the adding 5% of cold EGR in inlet air can decreases NOx by about half and insulating the engine increases the power and IMEP by about 7.7% and 8.5% and decreases the ISFC by about 7.5% at part load and increases power and IMEP by 8.5%, 8.5% and decreases ISFC by 8% at full load condition, respectively. Using this method, it was possible to control emissions formation and increase performance parameters simultaneously.

Keywords: air-cell, diesel engine, emission, injection, performance.

1. INTRODUCTION

Due to the growing importance of future emission restrictions and also fuel deficiency, improvement of engine performance and reduction of exhaust emissions have become important issues for automotive manufacturers. In order to improve the engine performance, the combustion process is now being studied in more detail. Also, the recent global environmental regulations for reducing engine emissions, designers' engine have forced to explore new engine concepts and to study the effect of engine parameters on the formation of pollutant emissions with more detail. Simulation of the combustion system by means of computer modeling makes it possible to explore combustion regimes that may be difficult and/or expensive to achieve with experiments [1].

Flow field models, such as KIVA II code in 1990 [2, 3] and numerical Ricardo Code in 1992 which were employed to investigate an optimum value for gas fuel injector angle in a dual fuel diesel-gas engine to obtain minimum UHC emissions [4], are premiere examples. Choi Wook, et al [5] used STARCD code and PIV analysis to study in-cylinder flow field of a single cylinder DI diesel engine. It was indicated that high Reynolds turbulent model pretty much satisfies such flow fields.

Lots of experimental researches have been done to decrease Soot and NOx emissions simultaneously. Kawazoe and et al [6] have significantly reduced exhaust Soot emission using an air-plunger pump type air-jet generator into combustion chamber in a DI diesel engine. Nagano and et al [7] have studied an air-accumulation type air-jet generator to reduce exhausted NOx and Soot emissions. Choi and Foster [8] have utilized a high pressure gaseous injector to control mixing in-cylinder in a DI engine. To investigate the effects of the composition of injected gas, both nitrogen and carbon dioxide have been used as the gaseous medium.

[Downloaded from www.iust.ac.ir on 2025-07-18]

Because of opposite behavior of NOx and Soot production in combustion process, their simultaneous decreasing needs accurate study on the flow field in combustion chamber, mixture formation and their effects on the combustion process. Computational Fluid Dynamics (CFD) is one of the most efficient methods for this purpose.

Uludogan and et al [9] have explored the use of multiple injectors and split injection to reduce DI diesel engine emissions. They have shown multiple injectors increase engine power density and significantly reduce particulate and NOx emissions. Combining EGR with multiple injection system results reduced both NOx and Soot without negative effects on fuel consumption [10].

Mather and et al [11] have shown that the utilizing an air-cell created inside the piston, improves the fuel-air mixing and reduces Soot emission from diesel engine without increasing the emission of NOx . Their results indicated that it can be an effective way to reduce particulate emissions by increasing mixing during the late combustion period with an air-jet injected into the main combustion chamber. In this study reduction of particulate by as much as a factory of two was observed with a simultaneous, but slight, reduction in NOx . E.M.Kurtz and et al [12] experimentally have studied the effects of increased in cylinder mixing on emission in diesel engine. Volker Joergl,Michael Becker experimentally have studied the effect of air injection and EGR on the emission in a single cylinder passenger cars and they showed that the emission can be improved by this work[13].

In order to increases thermal efficiency and improves operation characteristics engine such as power, SFC and MEP, reducing the amount of energy rejection from an internal combustion engine is essentially. In a conventional internal combustion engine, approximately one-third of total fuel input energy is converted to useful work. Since the working gas in a practical engine cycle is not exhausted at ambient temperature, a major part of the energy is lost with the exhaust gases. In addition, another major part of energy input is rejected in the form of heat loss via the cooling system. If the energy normally rejected to the coolant could be recovered on the crankshaft as useful work, then a substantial improvement in fuel economy would result.

The major investigations about the low heat rejection (LHR) engines for achieving high performance engines have been done by Bryzik and Kamo [14-17]. Van Sudhakar [18] has studied the development of the adiabatic diesel engine with the goal of 65% reduction in net in-cylinder heat transfer over a cooled engine and several un-cooled engines with intermediate levels of reduced heat transfer. The engine performance and exhaust emissions are also measured and compared.

Kawamura et al [19] have improved combustion process in a LHR diesel engine using a centrally located pre-combustion chamber in the cylinder head and throat holes drilled in it as radiating to cylinder inner surface. It is realized about 10% improvement in fuel economy compared to conventional DI diesel engine. Cheng and et al [20] have compared heat transfer characteristics in insulated and non-insulated diesel engines at the same speeds, loads and air-flow rates. Compared to the baseline engine, the insulated engine had a higher BSFC which was attributed to a slower combustion process.

Rakopoulos and et al [21] have simulated combustion process in chamber insulation using a multi-zone model and investigated its effects on the performance and exhaust emissions. It is found that the rising heat insulation leads to a significant increase of the exhaust NOx and a moderate increase of the exhaust Soot concentration. The more detail about ceramics characteristics which are utilize in LHR engines are experimentally investigated in [22-25].

As can be seen in the relevant literature, few studies seem to have been performed recently about simultaneously improvement of performance and emission for DI engines. At the Present work, intended for a contribution to the open literature, a CFD code has been utilized to numerically investigate the simultaneous effects of creating an air-cell inside the piston, adding EGR to the inlet air and insulating the combustion chamber walls on the combustion process, operation characteristics and exhaust emissions formation at both part (75% of full load) and full load conditions.

2. INITIAL AND BOUNDARY CONDITIONS

Calculations are carried out on the closed system from intake valve closure (IVC) at 147°CA BTDC to exhaust valve opening (EVO) at 100°CA ATDC. Figure 1 shows the numerical grids for the baseline (Caterpillar 3401) and baseline with air-cell created

[Downloaded from www.iust.ac.ir on 2025-07-18]

engines, which are designed to model the geometry of the engine. The volume clearance and also the compression ratio in both geometries are the same. Considering the symmetry of the model, problem is only solved for a 60 degrees section (6 holes injector) and contains a maximum of 21500 cells at 147°CA BTDC. The present resolution was found to give adequately grid independent results. Utilizing symmetry geometry has negligible error in the study of real engine parameters (piston head, off-centric injector and etc.) [26]. Initial pressure in the combustion chamber is set to be 200kPa and initial temperature is calculated to be 344K, and swirl ratio is assumed to be on quiescent condition for all cases. This study has been performed at 1600rpm constant engine speed for two different load (75% of full load and full load) conditions. In the cases with insulated walls, the boundary condition is assumed to be adiabatic wall and in the non-insulated cases, all boundaries temperatures were supposed to be constant throughout the simulation, but allowed to vary with the combustion chamber surface regions.

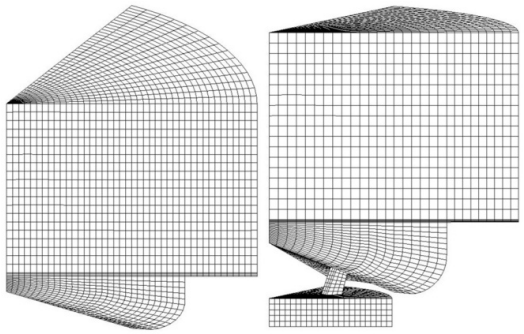

(a) (b)

Fig. 1. Computational geometries for (a) baseline engine (Caterpillar 3401) and (b) air-cell created engine

3. MODEL FORMULATION

The numerical model is carried out for the Caterpillar 3401 direct injection diesel engine with the specifications on the table 1. The governing equations for unsteady, compressible, turbulent reacting multi-component gas mixtures flow and thermal fields were solved from IVC to EVO by the AVL Fire CFD code [27]. The turbulent flows within the combustion chamber are simulated using the RNG k- ε turbulence model, modified for variable-density engine flows [28].

Table 1. Specifications of Caterpillar 3401 DI diesel engine

Cycle Type	Four Stroke
Number of Cylinders	6
Injection Type	DI
Cylinder Bore	137.6 mm
Stroke	165.1 mm
Displacement Volume	2.44 lit.
Compression Ratio	15.1 : 1
Engine Speed	1600 rpm
Full Load Injected Mass	16.22 g per Cycle
75% of Full Load Injected Mass	12.165 g per Cycle
Injection Pressure	90 MPa
Start Injection Timing	8.5 CA BTDC
Nuzzle Diameter at Hole Center	3 mm
Number of Nuzzle Holes	6
Nuzzle Outer diameter	0.259 mm
Spray Cone Angle	10°

At the present study because of high pressure injection system (common rail) standard WAVE break up model [29] is used for the primary and secondary atomization modeling of the spray and resulting droplets. Also drop parcels are injected with characteristic size equal to the Nozzle exit diameter (blob injection).

The Dukowicz model is applied for treating the heat up and evaporation of the droplets, which is described in [30]. A Stochastic dispersion model was employed to take the effect of interaction between the particles and the turbulent eddies into account by adding a fluctuating velocity to the mean gas velocity [27]. This model assumes that the fluctuating velocity has a randomly Gaussian distribution. The spray/wall interaction model used in this simulation was based on the spray/wall impingement model [31].

The Shell auto-ignition model was used for modeling of the auto ignition [32]. In this generic mechanism, 6 generic species for hydrocarbon fuel, oxidizer, total radical pool, branching agent, intermediate species and products were involved. In addition the important stages of auto ignition such as initiation, propagation, branching and termination were presented by generalized reactions, described in [27, 32].

The Eddy Break-up model (EBU) based on the turbulent mixing was used for modeling of the combustion in the combustion chamber [27] as follows:

[Downloaded from www.iust.ac.ir on 2025-07-18]

$$\overline{\rho \dot{r}_{fu}} = \frac{C_{fu}}{\tau_R} \bar{\rho} \min\left(\bar{y}_{fu}, \frac{\bar{y}_{ox}}{S}, \frac{C_{pr} \cdot \bar{y}_{pr}}{1+S} \right) \quad (1)$$

Where this model assumes that in premixed turbulent flames, the reactants (fuel and oxygen) are contained in the same eddies and are separated from eddies containing hot combustion products. The rate of dissipation of these eddies determines the rate of combustion. In other words, chemical reaction occurs fast and the combustion is mixing controlled. The first two terms of the "minimum value of" operator determine whether fuel or oxygen is present in limiting quantity, and the third term is a reaction probability which ensures that the flame is not spread in the absence of hot products [27]. Above equation includes three constant coefficients (C ,τ , C) and C_{fu} varies from 3 to 25 in diesel engines. An optimum value was selected according to experimental data [9, 34].

NOx formation is modeled by the Zeldovich mechanism and Soot formation is modeled by Kennedy, Hiroyasu and Magnussen mechanism [33].

4. RESULTS AND DISCUSSION

In the present work, firstly the air-cell has been created inside the piston and then the main combustion has been insulated while the initial volume of combustion chamber is constant. The volumetric ratio of air-cell is selected as 16% of volume clearance that which is optimized volume according to reference [11]. Finally the cold EGR effects are investigated by adding 5 and 10 mass fractions to the inlet air. The numerical results of others EGR mass fractions show that improvement in performance and emissions are not achieved for these cases. The operating conditions are 75% of full load and full load at constant speed of 1600 rev/min.

Figure 2 shows the comparison of predicted and experimental in-cylinder pressure for both part and full load conditions for baseline engine. The results presented in this figure are global (cylinder averaged) quantities as a function of time (crank angle). The good agreement between measured and predicted data especially during the compression and expansion strokes with the start of combustion time verifies the result of model. The peak pressures discrepancy between experiment and computation is less than 1%. Figure 2 also shows the quantity of computational and experimental results for Start of Combustion (SOC) and Ignition Delay (I.D) crank angle degrees in both cases. The discrepancies of SOC or I.D between computation and experiment at part load and full load operation are as small as 1 and 2CA respectively.

This verification for baseline and baseline with air-cell states demonstrate that multidimensional modeling can now be used to gain insight into the combustion process and to provide direction for exploring new engine concepts.

Figure 3 indicates the pressure histories for the baseline engine, insulated baseline, insulated and air-cell connected case with 5% and 10% EGR added to the final modified case at two loads. It is obvious that peak pressure will increase by increasing the engine load. At this type of engine, increasing the load from 75% to the full load is caused to increase the peak pressure by about 15% in all cases (comparison between figures 5.a and 5.b). Also increasing the load

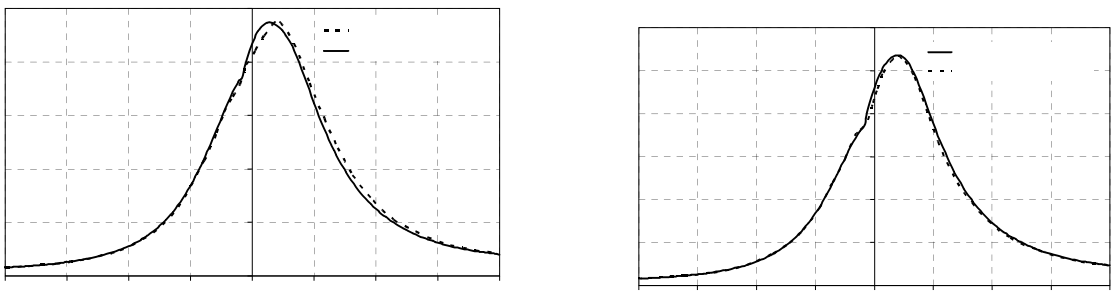

(a) 75% of full load (b) Full load

Fig. 2. Comparison of predicted and measured engine in-cylinder pressure for the Caterpillar diesel engine at (a) 75% of full load and (b) full load condition at 1600rpm

[Downloaded from www.iust.ac.ir on 2025-07-18]

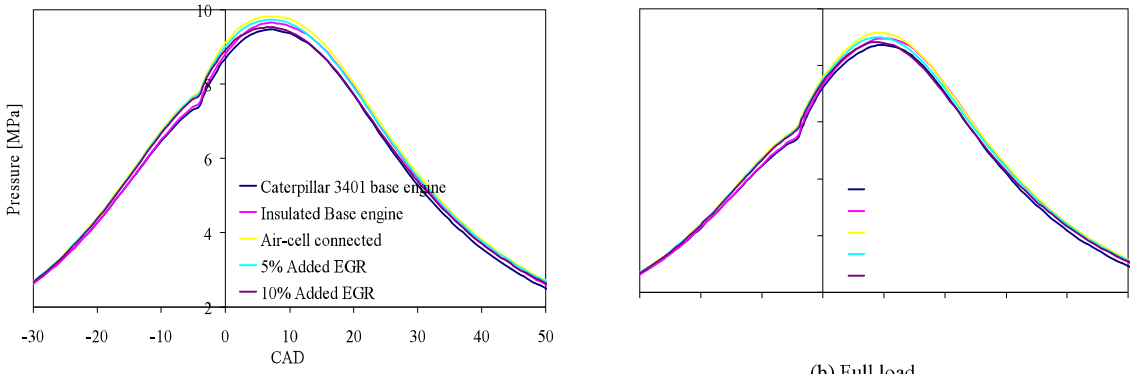

(a) 75% of full load (b) Full load

Fig. 3. Mean in-cylinder pressure versus crank angle for (a) 75% of full load and (b) full load conditions

had no debatable effect on ignition delay and start of combustion. The peak pressure occurs at 7CA ATDC at 75% of full load and 10CA ATDC at full load condition. The insulation, air-cell creating and EGR applying have no considerable effect on peak pressure occurrence point.

By insulating the baseline engine because of no heat loss from the cylinder and piston walls, the peak pressure increases by about 1.5% and 2.5% at both part and full loads, respectively as can be seen in figures 4. Creating the air-cell under the piston head which connected to the mean combustion chamber with rectangular throat increases the cylinder pressure by about 1.9% and 1.6% at both part and full load conditions, respectively. As it is shown these figures that initial pressure for air cell case was elevated slightly above the initial condition for standard engine. This change in initial condition was required for air cell equipped engine to match the temperature and pressure at the start of injection of standard engine.

Adding EGR to the air inlet because of decreasing air available for combustion in the main chamber also increasing thermal capacity causes the peak pressure decreases. Increasing the EGR mass fraction more decreases the peak pressure.

Figure 4 indicates the mean temperature histories versus crank angle for both part and full load conditions. Increasing the engine load from 75% of full load to the full load condition increases the peak temperature by about 250-300K and exhaust temperature by about 200-250K. The peak temperatures in all cases occur at 25CA ATDC.

Insulating the combustion chamber results to reduce the heat loss from the cylinder walls and increases the in-cylinder peak temperature by about 150K in both part and full load conditions. The maximum exhaust temperature occurs in air-cell cases because of resuming combustion in late combustion period. Due to decreasing the in-cylinder pressure at expansion stage, the reserved air in the air-cell injects to the main

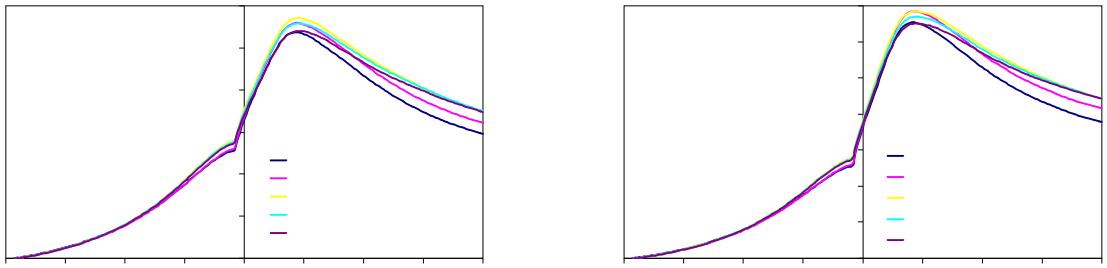

(a) 75% of full load (b) Full load

Fig. 4. Mean in-cylinder temperature versus crank angle for (a) 75% of full load and (b) full load conditions at 1600rpm

[Downloaded from www.iust.ac.ir on 2025-07-18]

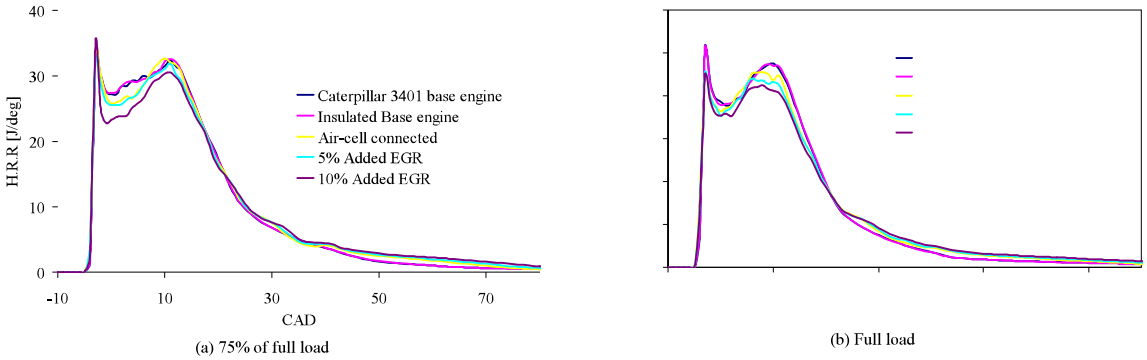

Fig. 5. Rate of heat release versus crank angle for (a) 75% of full load and (b) full load conditions

chamber and combusts the remaining fuel. Adding EGR to the air inlet decreases the peak temperature.

A match of pressure and temperature behaviors of all cases would imply that the spray vaporization, ignition and combustion characteristics of standard engine and the air cell equipped engine would be similar [11].

Heat release rate curves are shown in figure 5 for both part and full load operation conditions. Increasing load to full load mode causes ignition delay decreased to 5CA from 6 CA with respect to 75% load. Figure 6 indicates that converting the constant temperature boundary condition to the insulated walls, creating the air-cell inside the piston and also adding EGR have no debatable effect on ignition delay.

This means that the effects of decreasing oxygen concentration and increasing heat capacity on ignition delay is equal the increased charge temperature when engine is insulated.

The value of premixed burning phase slightly increases due to insulating the walls and decreases due to increasing EGR, and air-cell has no sizeable effect on it. At the start of diffusion burning phase (near TDC) in air-cell connected cases because of the lack of air in main chamber, burning rate is slow and increasing EGR makes it slower. The causes of fast burning rate from near TDC to 10CA ATDC (as shown in figure 5) pertain to high temperature regions indicating significant heat release rate within air cell and the decreased resistance to flow into the air cell by changing the turbulence levels at the inlet passage[11] . One feature of heat release rate traces for the air-cell engine is the rise in heat release rate that can be seen near 10 after TDC at part and full loads. The reason of this rise is that the fuel injection influences the in-cylinder flow filed. Eventually, when the spray reaches the air-cell passage, the flow produced by the fuel injection interacts with the flow into the air-cell flow beginning to reverse direction and emerge out of the air-cell at +10 ATDC [11].

But in the late combustion period (after 20CA ATDC), while the reserved air in air cell injects to the main chamber, combustion continues until almost exhaust valve opening. This combustion has a very vital effect on Soot reduction.

Also according to figure 5, insulation causes that premixed burning fraction increase and a corresponding in the amount of diffusion burning fraction decreases.

5. PERFORMANCE PARAMETERS

Table 2 shows the variation of performance parameters including net cycle work, indicated power, mean effective pressure (IMEP) and specific fuel consumption (ISFC) versus load operation conditions in all cases. Indicated work per cycle was calculated from the cylinder pressure and piston displacement, as follows:

$$W = \int_{\theta}^{\theta} PdV \tag{2}$$

Where $\theta 1$, $\theta 2$ are the start and end of the valve closed period, respectively (i.e. IVC= -147CA BTDC and EVO= 100CA ATDC). The indicated power per cylinder and indicated mean effective pressure were related to the indicated work per cycle by:

$$P(KW) = \frac{W(N.m)N(rpm)}{60000n} \tag{3}$$

[Downloaded from www.iust.ac.ir on 2025-07-18]

Table 2. Operation characteristics for all cases at both part and full load conditions

		Work [kJ/cycle]	Indicate Power [kW]	$\dot{m}_{fuel}$ [g/sec]	IMEP [Bar]	ISFC [g/kW.h]
Part load condition	Caterpillar 3401 base	2.0	26.64	1.62	8.15	291.92
	Insulated Base engine	2.17	28.92	1.62	8.84	269.09
	Air-cell connected	2.27	30.30	1.62	9.25	257.02
	5% Added EGR	2.24	29.82	1.62	9.11	261.12
	10% Added EGR	2.16	28.80	1.62	8.80	270.17
Full load condition	Caterpillar 3401 base	2.72	36.18	2.16	11.06	215.07
	Insulated Base engine	2.94	39.24	2.16	12.00	198.25
	Air-cell connected	3.02	40.32	2.16	12.32	193.08
	5% Added EGR	2.97	39.60	2.16	12.10	196.56
	10% Added EGR	2.90	38.70	2.16	11.82	201.24

$$IMEP = \frac{W}{V_d} \tag{4}$$

Where n= 2 is the number of crank revolutions for each power stroke per cylinder, N is the engine speed, rpm, and is volume displacement. The brake specific fuel consumption (BSFC) was defined as:

$$ISFC = \frac{\dot{m}_f}{P_i} \tag{5}$$

In eqn. 2, the work was only integrated as part of the compression and expansion strokes and the pumping work was not taken into account. Therefore, the power and ISFC analyses can only be viewed as being qualitative rather than quantitative in this study.

With the increase of the engine load, net cycle work, indicated power and IMEP increase and ISFC decreases as expected. For both part and full load conditions, the obtained results for studied cases are the same.

Insulating the engine and creating the air-cell have positive effect on performance parameters. Insulating the base engine increases the indicated power and IMEP by about 7.7% and 8.5% at part load condition and 8.5% and 8.5% at full load condition respectively, also decreases the ISFC by about 7.5% and 8% at part and full load respectively. The effect of air-cell on performance parameters is lesser than insulation (about 3%). As can be seen in table 2, adding EGR to the inlet air has negative effect on engine performance.

6. EMISSION FORMATION RESULTS ANALYSIS

In the following section, the productions of NOx and Soot as main emissions in DI Diesel engines are discussed. In figure 6 the exhaust NOx and Soot quantities for the base engine at full load condition are compared and verified with experimental data [34]. There is a good agreement among the results.

In figures 7.a and 7.b are shown the NOx formation histories for all cases. As can be seen, increasing the operation load causes to increase the NOx emission as factor of two because of higher peak temperature and peak premixed combustion at full load condition (figures 4 and 5). NOx formation starts off at about 14CA for full load and 15CA for part load operation state after the start of injection. The initial increase in

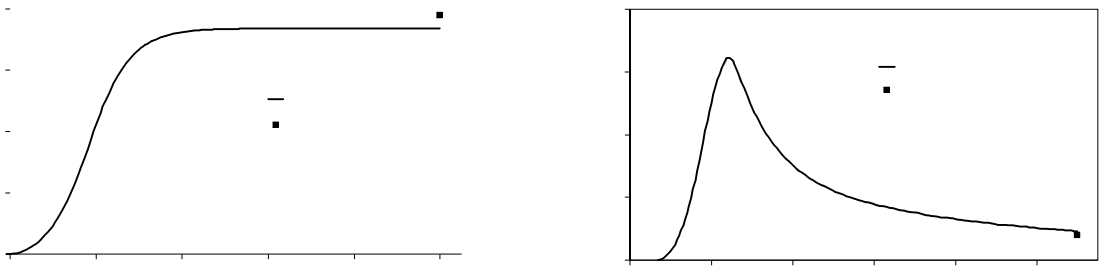

(a) NO pollutant (b) Soot pollutant

Fig. 6. Comparison of predicted and measured engine pollutants at full load condition and 1600rpm for the Caterpillar diesel engine

[Downloaded from www.iust.ac.ir on 2025-07-18]

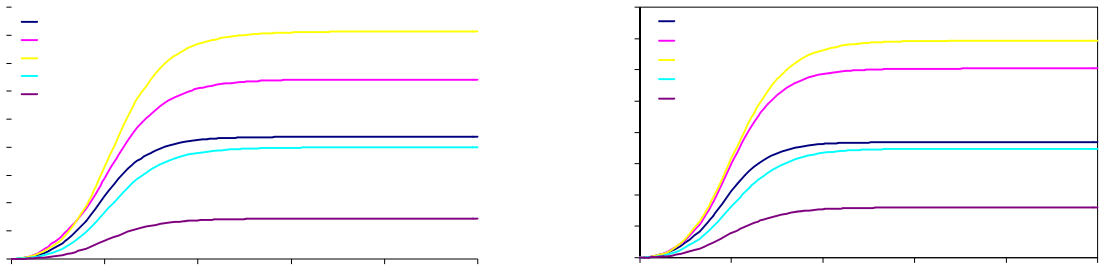

(a) 75% of full load (b) Full load

Fig. 7. Model results for NOx emission for all cases at (a) 75% of full load and (b) full load operation conditions at 1600rpm

the global NOx formation follows the global temperature trend (also on figure 6).

Insulating the combustion chamber walls causes to decrease the heat loss from the walls and increase the in-cylinder temperature and as a result of that NOx increases. Also creating the air-cell increases NOx emission. Insulating and connecting the air-cell increases the NOx as a factor of two in both part and full load conditions. Adding EGR to the inlet air is a very effective solution in NOx reduction because of decreasing the peak temperature in combustion chamber. As can be seen in figure 9, 5% of EGR reduces NOx by about half and 10% of EGR reduces this emission by about one fifth.

Figure 8 presents the evolution of the Soot formation in the combustion chamber for both load conditions. One could notice that at part load, the exhaust quantity of Soot is further than full load by about a factor of two. Soot emission attains its peak at near peak of diffusion phase of combustion and because of the availability of sufficient oxygen; the turbulent Soot oxidation diminishes the Soot concentrations. The Soot is then oxidized again in the leaner regions of the flame, so that most of the Soot is already consumed in zones close to the stoichiometric.

As can be seen on figure 8, insulating the chamber walls have no effect on exhaust Soot concentration. Creating the air-cell reserves some of the air at compression stage and due to decreasing the in-cylinder pressure at expansion stage, this air injects to the main combustion chamber. Injecting the low temperature air increases the Soot oxidation rate and reduces the exhaust Soot concentration. Adding EGR to the inlet air decreases the Soot oxidation rate and as a result of that exhaust Soot increases.

At whole, NOx formation is intensified in areas with equivalence ratio close to 1 and the temperature higher than 2000K. In addition to this, the area with the equivalence ratio higher than 3 (regions near to spray jet) and the temperature approximately between 1600K and 2000K, yields in greater Soot concentrations [35]. Under medium and high load conditions, the main cause of the exhaust smoke can be both the fuel adhesion to the chamber wall and

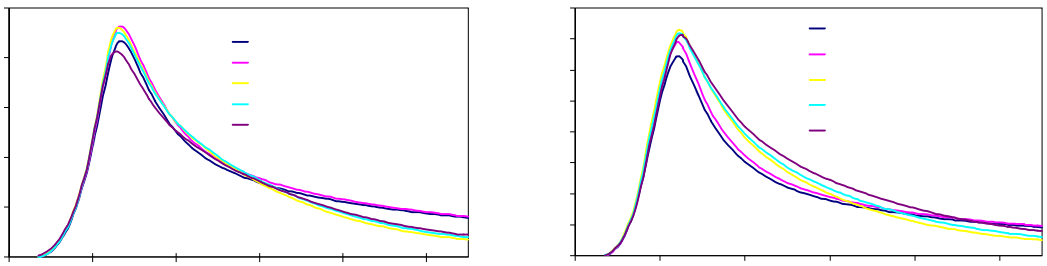

Fig. 8. Model results for Soot emission for all cases at (a) 75% of full load and (b) full load operation conditions

[Downloaded from www.iust.ac.ir on 2025-07-18]

stagnation of rich fuel-air mixture. NOx and Soot emissions have opposite formation procedure. In any combustion processes, reducing the NOx causes to increase the Soot.

At Figures 9 and 10 from left to right are shown the contours of the temperature, NOx, Oxygen, vapor mass fractions, Soot formation regions at state of base engine, adiabatic base engine, adiabatic air cell connected engine, adiabatic air cell connected engine with 5% and 10% EGR from top to bottom respectively in order to study combustion process and emission formation with zonal method. The regions with high temperature and sufficient oxygen mass fraction in the combustion chamber and air-cell are potential NOx producing regions. At ten degrees ATDC when the flow is just starting to reverse and flow out of the air-cell, the NOx contours show two regions of NOx, one in the lip bowl of main combustion chamber and the other in the air-cell at the stagnation region under the inlet channel to the air-cell. The two NOx regions may be either the result of two distinct ignition and combustion process, or by combustion gases forced into the air-cell where combustion and NOx production continues.

Heat conduction to the walls had a significant quenching action on the high temperature NOx producing regions inside the air-cell. Subsequent NOx contours in figure 10 (+40) show that while the air-cell is emanating a jet into the combustion chamber, the region of high NOx omitted inside the air-cell on the cylinder axis side of the passage. Adding EGR to the inlet air decreases the NOx producing in the air cell and adding air cell to base engine and also insulating increase NOx emission.

A demonstration of the effect of the air-cell on the Soot contours is seen by overlaying the vapor fuel

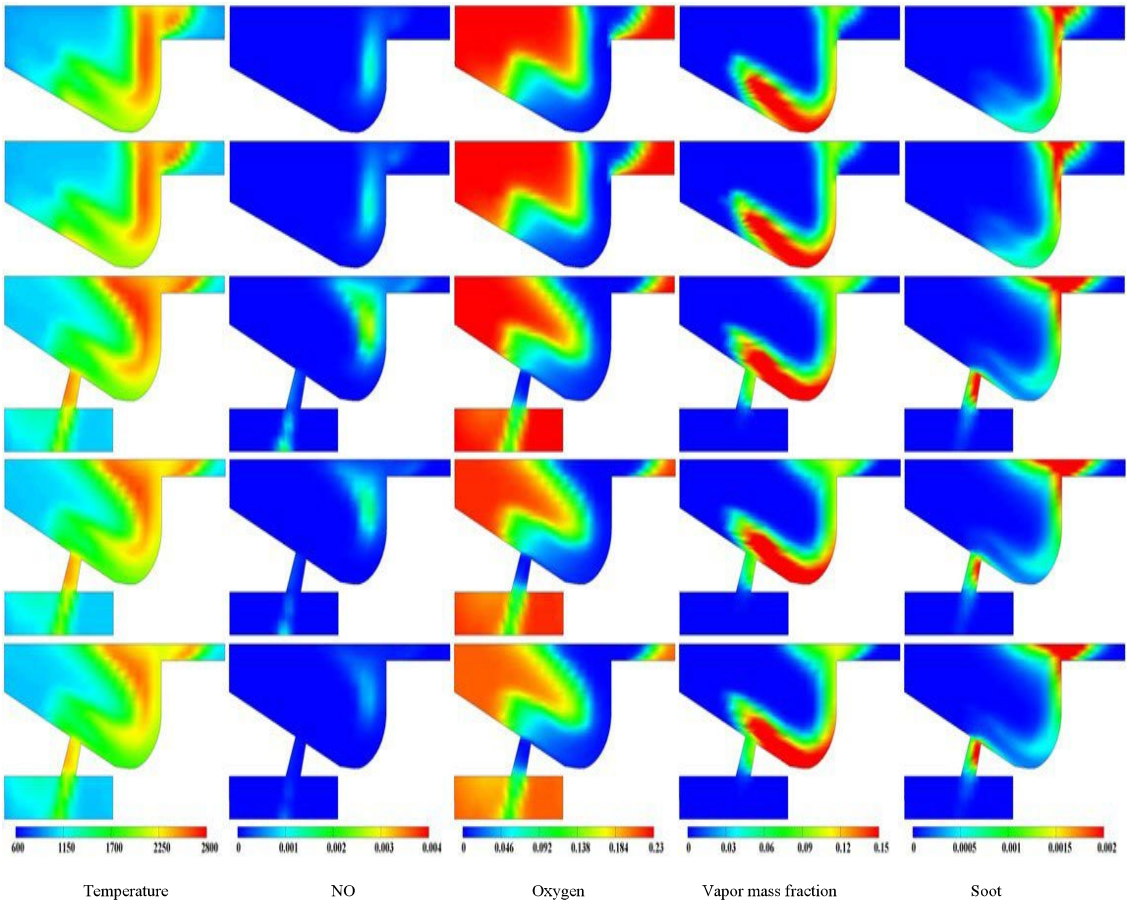

Fig. 9. NOx, Soot, temperature, Oxygen and vapor mass fractions contour plots at full load operation condition at 10CA ATDC and 1600rpm

[Downloaded from www.iust.ac.ir on 2025-07-18]

mass fraction, oxygen mass fraction and temperature contours plots at different cases. During the early part of combustion, Soot is forming in the main combustion chamber in high vapor mass fraction regions and gets drawn into the air-cell as the air-cell is charging (don't shown contours). However, the Soot that gets drawn into the air-cell is oxidized and negligible Soot is present in the air-cell at the time of flow reversal (+10 ATDC) while Soot which is forming in the back of air cell passage mouth, because of lack of oxygen ,less mixing is not oxidized. At this time the Soot in the main combustion chamber and air cell passage have been swept to the edge of the piston bowl by the flow field produced by the spray. As the air-jet emanating from the air-cell enters the combustion chamber the region of high Soot concentration region has moved to the rim of the piston bowl where the reverse squish flow velocity field. The air-jet emanating from the air-cell has crossed with the flow field of main combustion chamber and stretches the region of high Soot concentration (+40 ATDC) and causes augmenting mixing and increasing the rate of Soot oxidation. This period of the Soot oxidation being highly influenced by the air-jet corresponds to the period of rapid Soot oxidation for the air-cell engine and then Soot emission reduce to half than the baseline engine. As the simulation continues, the region of high Soot production is drawn down the side of the piston bowl under the influence of a recirculation flow zone produced by the air-jet. These figures clearly demonstrate the enhanced Soot/air mixing produced

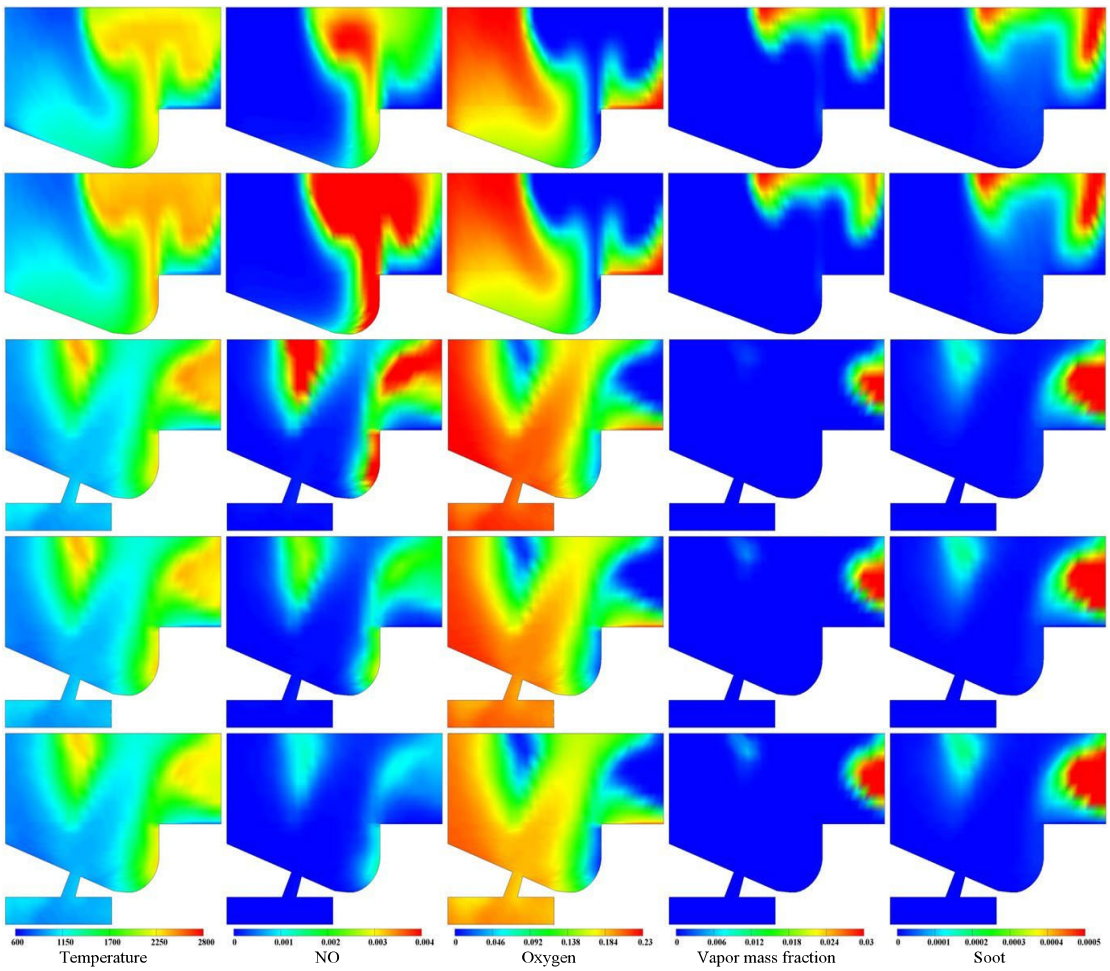

Fig. 10. NOx, Soot, temperature, Oxygen and vapor mass fractions contour plots at full load operation condition at 40CA ATDC and 1600rpm

[Downloaded from www.iust.ac.ir on 2025-07-18]

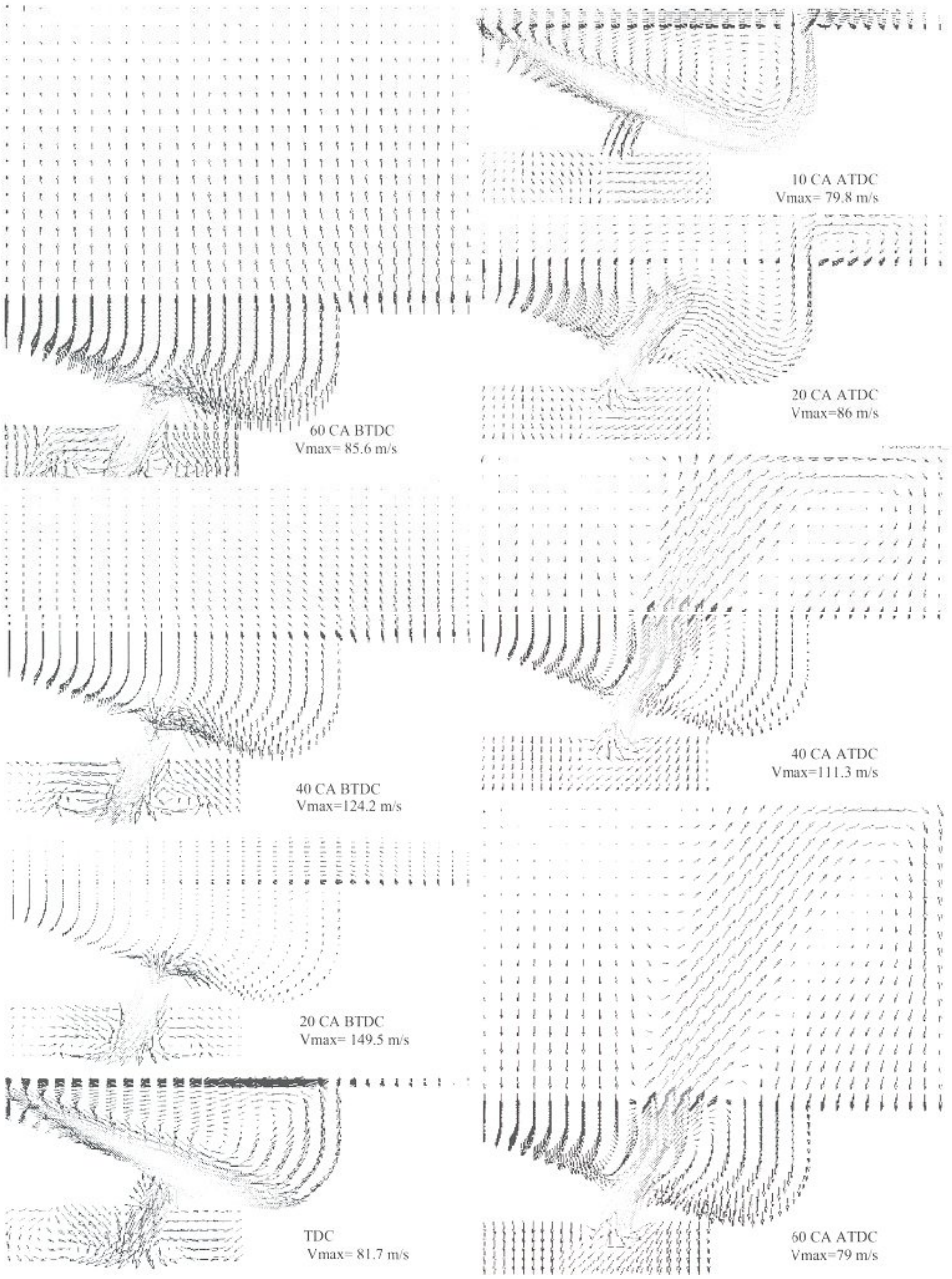

Fig. 11. Velocity vectors presenting the action of the air-cell at various crank angles at 1600rpm.

by the air-jet emanating from the air-cell. This enhanced mixing is responsible for the factor of two reductions in overall Soot production for the air-cell engine that which is seen in figure 8. Also adding EGR and insulation have no noticeable effect on exhaust Soot concentration.

A local Soot-NOx trade-off is evident in these contour plots where the NOx and Soot formation occur on opposite sides of the high temperature region [35].

Figures 11 show the action of the air-cell by presenting velocity vectors in a slice through the

[Downloaded from www.iust.ac.ir on 2025-07-18]

center of the sector mesh cutting down the center of the passage that joins the air-cell to the combustion chamber. All velocities in between the top of the piston and the head vary from the piston velocity to the head velocity that which is zero. Figure 11 (-60 BTDC) shows the evolution of the flow into the air-cell, which becomes the fully developed flow shown at-40, -20 BTDC respectively) with a recirculation zone forming inside the air-cell axis side of the passage. The appearance of large velocity vectors in the main combustion chamber at TDC and 10 ATDC seen in this figure shows the fuel injection (11 BTDC SOI) starting to influence the in-cylinder flow. Eventually, when the spray reaches the air-cell passage, the flow produced by the fuel injection interacts with the flow into the air-cell, (TDC). The flow beginning to reverse direction and emerge out of the air-cell as shown in this figure at 10 ATDC. At 20 and 40 ATDC, the jet emanating from the air-cell piercing through the flow produced by the fuel injection. Figure 11 (40 ATDC) shows the jet at its maximum exit velocity of 111.3 m/s, significantly influencing the flow across the entire combustion chamber to the engine head. This flow pattern is maintained though the end of the simulation at 60 ATDC.

7. CONCLUSIVE REMARKS

In this paper, at the first step combustion processes, pollutant formation, and the operation characteristics within Caterpillar 3401 DI Diesel engine were simulated at full load and part load operation conditions. The results for calculated pressure exhaust emissions and performance parameters were compared with the corresponding experimental data and show good agreement. Such verification between the experimental and computed results gives confidence in the model prediction, and suggests that the model may be used at future works. At the second step of CFD simulation in order to improve of performance and emissions at the modified engine, insulating and EGR applying method are used. At the result of this step, it was shown that insulating the combustion chamber walls improves the operation characteristics, creating the air-cell decreases the exhaust Soot concentration and adding EGR to the inlet air reduces the NOx emission. Comparing the finally modified case (insulated, air-cell connected and 10% of EGR added to the air inlet) to the base caterpillar engine indicates that the power and IMEP are increased by about 7% and 6.8%, ISFC is decreased by about 6.4%, and Soot and NOx emissions are reduced by about 50% and 60%.

REFERENCES

[1] A. Uludogan, D. E. Foster, and R. D. Reitz “Modeling the Effect of Engine Speed on the Combustion Process and Emissions in a DI Diesel Engine”, SAE paper 962056.

[2] J. B. Heywood, “Internal combustion engine fundamental.” McGraw Hill Book Company, New York, 1988.

[3] A. D. Gosman. “Computer modeling of flow and heat transfer in engines, progress and prospects”, Imperil College of Science and Technology, London, 1985.

[4] R. Jeske Felix, etc., “Modeling of the natural gas injection process in a two-stroke diesel engine”, SAE Paper 920192.

[5] Choi Wook, etc., “In-cylinder flow field analysis of a single cylinder DI diesel engine using PIV and CFD”, SAE Paper 2003-01-1846.

[6] Kawazoe, H. Nagano, S. and Ohsawa K., “Reduction of Soot Emission by Air-Jet Turbulence Generator with Cam in a Diesel Engine”, JSAE Review, Vol. 12, No. 3, 1991.

[7] Susumu Nagano, Hiromitsu Kawazoe, and Katsuyuki Ohsawa, “Reduction of Soot Emission by Air-Jet Turbulence in a DI Diesel Engine”, SAE Paper 912353, 1991

[8] C. Y. Choi, D. E. Foster, “In cylinder augmented mixing through controlled gaseous jet injection”, SAE Paper 952358, 1995

[9] A. Uludogan, J. Xin, R. D. Reitz," Exploring the use of multiple injectors and split injection to reduce DI diesel engine emissions," SAE Paper 962058, 1996

[10] R. D. Reitz, D. T. Montgomery, “Six-mode cycle evaluation of the effect of EGR and multiple injections on particulate and NOx emissions from a D.I. diesel engine," SAE Paper 960316, 1996

[11] D. K. Mather, R. D. Reitz, " Modeling the use of air-injection for emissions reduction in a direct-injected diesel engine," SAE Paper

[Downloaded from www.iust.ac.ir on 2025-07-18]

952359, 1995.

[12] E. M. Kurtz, D. E. Foster "Identifying a critical time for mixing in a direct injection diesel engine through the study of increased in-cylinder mixing and its effect on emissions", International Journal of Engine Research, June 1, 2004; vol. 5, 3: pp. 247-256.

[13] V. Joergl, M. Becker "Application of Concentric Cam Shafts to a Passenger Car Diesel Engine to Significantly Improve the NOx /Soot Tradeoff",SAE paper 2011-24-0134,2011.

[14] R. Kamo, W. Bryzik, "Cummins/Tacom Advanced Adiabatic Engine", SAE Paper 840428, 1984

[15] W. Bryzik, R. Kamo, "Tacom/Cummins Adiabatic Engine Program", SAE Paper 830314, 1983

[16] R. Kamo, W. Bryzik, "Ceramics in Heat Engines", SAE Paper 790645, 1979

[17] R. R. Sekar, R. Kamo, J. C. Wood, "Advanced Adiabatic Diesel Engine for Passenger Cars", SAE Paper 840434, 1984

[18] V. Sudhakar, "Performance Analysis of Adiabatic Engine", SAE Paper 840431, 1984

[19] Hideo Kawamura, Akira Higashino, Shigeo Sekiyama, "Combustion and Combustion Chamber for a Low Heat Rejection Engine", SAE Paper 960506, 1996

[20] W. K. Cheng, V. W. Wong, F. Gao, "Heat Transfer Measurement Comparisons in Insulated and Non- Insulated Diesel Engines", SAE Paper 890570, 1989

[21] Robert E. Hetrick, Larry W. Cathey, "Vibrational Sensor Based on Fluid Damping Mechanisms", SAE Paper 900489,1990

[22] Ekrem Buyukkaya, Muhammet Cerit, "Thermal analysis of a ceramic coating diesel engine piston using 3-D finite element method", Surface & Coatings Technology 202 (2007) 398–402

[23] D. Assanis and K. Wiese, E. Schwarz, W. Bryzik, "The Effects of Ceramic Coatings on Diesel Engine Performance and Exhaust Emissions", SAE Paper 910460, 1991

[24] I. TaymazT, K. C¸ akVr, A. Mimaroglu, "Experimental study of effective efficiency in a ceramic coated diesel engine", Surface & Coatings Technology 200 (2005) 1182– 1185

[25] Yiming Wang, Changlin Yang, Guocai Shu, Yincheng Ju, Kuihan Zhao, "An Observation of High Temperature Combustion Phenomenon in Low-Heat-Rejection Diesel Engines", SAE paper 940949, 1994

[26] Zh. Liu and X. Gui "Investigation of Effects of Piston Bowl and Fuel Injector Offsets on Combustion and Emissions in D.I. Diesel Engines" International Truck and Engine Corp. SAE paper 2002-01-1748.

[27] AVL FIRE user manual V. 8.5; 2006.

[28] Han Z., Reitz R. D., “Turbulence Modeling of Internal Combustion Engines Using RNG K-e Models”, Combustion Science and Technology, Vol. 106, pp.267-295., 1995.

[29] Liu A B, Reitz R D., “Modeling the effects of drop drag and break-up on fuel sprays”, SAE Paper NO. 930072; 1993.

[30] Dukowicz JK., “Quasi-steady droplet change in the presence of convection”, informal report Los Alamos Scientific Laboratory. LA7997-MS.

[31]. Naber JD, Reitz RD., “Modeling engine spray/wall impingement”, SAE Paper NO. 880107, 1988.

[32] Halstead M, Kirsch L, Quinn C., “The Auto ignition of hydrocarbon fueled at high temperatures and pressures - fitting of a mathematical model”, Combustion Flame 30 (1977): 45-60.

[33] Patterson M. A., Kong S. C., Hampson G. J. Reitz R. D., “Modeling the Effects of Fuel Injection Characteristics on Diesel Engine Soot and NOx Emissions”, SAE Paper 940523, 1994.

[34] A. R. Binesh, and S. Hossainpour, “Three Dimensional Modeling of Mixture Formation and Combustion in a Direct Injection Heavy-Duty Diesel Engine”, International Journal of Mechanical, Industrial and Aerospace Engineering 2:4 2008.

[35] C. Baumgarten, “Mixture formation in internal combustion engines”, Springer publications 2006.

[Downloaded from www.iust.ac.ir on 2025-07-18]